Astronomical Image Processing: Galaxy Count from a KPNO Deep Optical Image

Dakshina Scott

November 4, 2012

Abstract

Galaxy counts were conducted on a deep optical image taken using the 4m telescope at KPNO with a Sloan r-band filter. This was done to test the relationship between galaxy number counts and magnitude, as predicted by the equation $log_{10}N(m) \propto 0.6m$.

A script was written in Matlab to detect galaxies within the image and catalogue their brightnesses. A plot of galaxy counts against magnitude was found to differ significantly from a similar survey, and from the above equation; the steepest gradient was found at the lower magnitudes to be 0.35 ± 0.02 (from magnitude 9.2 to 13). This deviation is thought to be due to incompleteness in the image rather than evidence of strong galaxy evolution or the structure of the universe.

1 Introduction

Galaxy surveys allow us to probe the history and structure of the universe. Number counts and photometric and spectroscopic analysis from such surveys have transformed our understanding of the universe - when in 1917 Einstein's theory of general relativity suggested that the universe must be either expanding or contracting, he brushed the idea aside. It was only after Silpher and Hubble produced data from galaxy surveys relating redshift and distance that the evidence in support of an expanding universe became impossible to ignore[2].

In this experiment we have looked at a deep optical image taken using a Sloan r-band filter (central wavelength 620nm) using the CCD mosaic camera at Kitt Peak National Observatory. The aim was to find the number counts of galaxies at different magnitudes, and compare our results to the prediction for an Euclidean universe of galaxies, with no evolution, described by equation 8. We also compared our counts to a similar survey with very high completeness in order to evaluate our method and our data.

By assuming an Euclidean universe of uniformly distributed galaxies, with a given distribution of luminosities, a simple relationship between magnitude and number of galaxies brighter than that magnitude can be derived. For a given luminosity distribution $f \propto \frac{1}{r^2}$ and so

$$r \propto \frac{1}{f^2}. \tag{1}$$

For a given density in Euclidean space

$$N \propto r^3. \tag{2}$$

Substituting equation 1 into equation 2 we get

$$N(f) \propto f^{-\frac{3}{2}} \tag{3}$$

where N(f) is the number of sources with flux greater than f.

Using

$$m_1 - m_2 = -2.5log_{10}(\frac{f_1}{f_2}), \tag{4}$$

the standard equation relating the difference in magnitude between two objects and the flux received from them, it can be seen that

$$m \propto -2.5log_{10}(f). \tag{5}$$

Rearranging for f

$$f \propto 10^{-2.5m}, \tag{6}$$

and substituting equation 6 into equation 2

$$N(m) \propto 10^{0.6m}. \tag{7}$$

Finally, taking the log of both sides

$$log_{10}(N(m)) \propto 0.6m \tag{8}$$

where N(m) is the number of sources brighter than magnitude m.

Based on this result, the difference in the number of galaxies between each magnitude is given by

$$N(m+1) = 4.0N(m). \tag{9}$$

However, the Friedmann equations tell us that the universe is not necessarily Euclidean; there may be a distance beyond which its structure influences galaxy counts.

In 1961 Sandage [8] found that galaxy counts from the Hale telescope (the world's largest telescope at the time[9]) were unlikely to reveal information about the structure of the universe because the differences between flat, open, and closed models are too small compared to known variations in galaxy distribution. On the other hand it was found that a magnitude-redshift relation may be more revealing. More recently Eisenstein et al (2001)[6] also found that the Sloan Sky Digital Survey would be well suited to studies of large-scale structure by making use of spectroscopic data.

One of the key results looked at in galaxy surveys (eg Maddox et al. 1990)[4] has been how the data deviates from the counts expected by a no-evolution model of galaxies - the further away the galaxy, the further in the past we are looking - so if for example galaxies were brighter/dimmer or more/less numerous, then distant galaxies may give counts inconsistent with equation 8.

Thus it is possible that comparing number counts against magnitude with the prediction of equation 8 will show evidence of galaxy evolution, but it is unlikely that effects of large-scale structure will be seen.

2 Method

Although the image had been processed to adjust for certain effects before it was received, there were still some unwanted effects remaining. Image processing and analysis was done in Matlab, with the image processing toolbox installed.

2.1 Noise

The image consists of a combination of a number of sub-exposures. This smooths out random noise, as inconsistent sources will be faded. It can be seen that these sub-exposures don't overlap exactly - as a result there are blank areas in the corners of the image, and around the edges a sharp increase in noise is visible (figure 1).

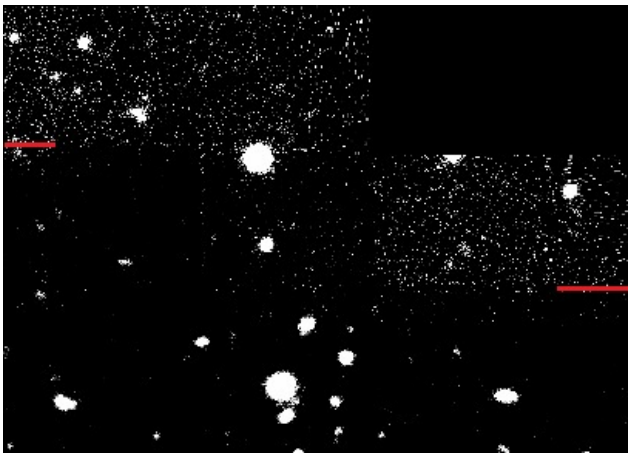

Figure 1: The red lines highlight sharp increases in noise where sub-exposures don't overlap. The top right corner is blank.

The image was cropped before analysis to remove the noisiest areas.

2.2 Saturated Pixels

'Blooming' is when pixels in the CCD are saturated and overflow to nearby pixels. This happens mostly in the vertical and horizontal directions, as seen in figure 2.

The maximum number of electrons each pixel of the CCD can hold is 65,535. For values approaching this, the relationship between number of photons received and the number of electrons stored moves further and further from one-to-one. By using multiple shorter exposures any given CCD pixel receives fewer photons, so the number of sources bright enough to cause overflowing is reduced. However this effect is still visible in some areas (highlighted in figure 2). These sources and their bloom were blacked out before analysis.

On this fully prepared image, two different algorithms for source detection and photometry were applied, each with different limitations. One method uses a fixed aperture, while the other uses the shape and size of each source to analyse the correct areas of the image. Both methods are dependent upon finding a suitable value for the source/background threshold.

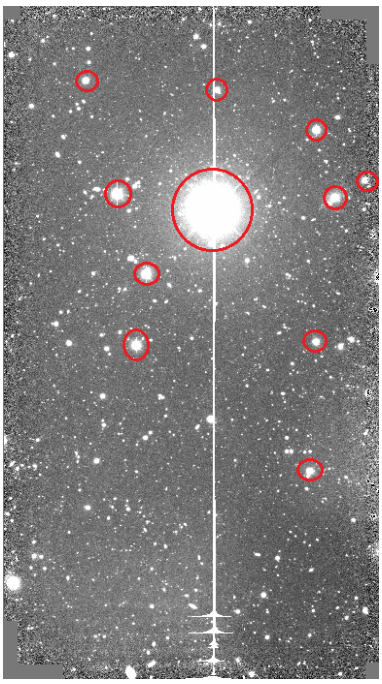

Figure 2: A bright central source which has 'bloomed' vertically across the image. There are also smaller sources showing the same effect to a lesser extent. Red circles indicate sources which were blacked out prior to analysis. The lines of bloom were also blacked out.

2.3 Finding an Upper Limit for Background Brightness

In order to analyse each source, some criterion must be used to determine how high a photon count must be in order for it to be considered to be coming from a source, rather than a background fluctuation. The image is composed mostly of background, with a scattering of sources of varying brightness. Thus the mode pixel value in the image gives an estimate of the background value. However, as the background isn't a constant value it's clear that much of the background will have values higher than this, and some upper limit of counts must be chosen as the threshold. Inspecting the distribution of photon counts within the image shows that the frequency of counts per pixel in the region of the modal value is many orders of magnitude greater than that for other values found in the image, and the distribution within this region is approximately Gaussian (figure 3). Thus a threshold value was chosen as three standard deviations above the mean in this region (a value of 3461 counts).

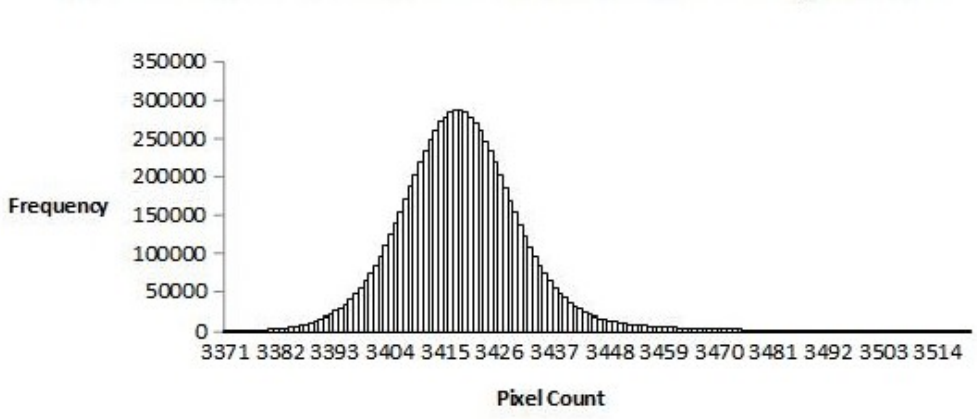

Figure 3: Histogram showing the Gaussian-like distribution of pixel counts in the region of the global background.

2.4 Fixed Aperture Method

Sources are identified and analysed using a fixed aperture size. The maximum pixel value in the image is found, and the surrounding area analysed. This area is then blacked out so that a search for the new maximum will find the second-brightest source from the original image, which is then analysed, and so on. This continues looping around until the maximum remaining value equals the threshold value.

A number of different aperture sizes were tried in an attempt to find a compromise between a very large and a very small aperture. Any source larger than the chosen aperture size ends up with a lower count attributed to it than it should have, reduced even further when the 'local background' (which in this case will at least partially be obscured by the source) is subtracted. Also, the smaller the aperture the more opportunity there is for each source to be counted as multiple sources (although measures were taken within the code to reduce this - see figure 4). Sources which are smaller than the aperture will have a reduced mean intensity value, although the total number of counts should be about right once the local background has been subtracted.

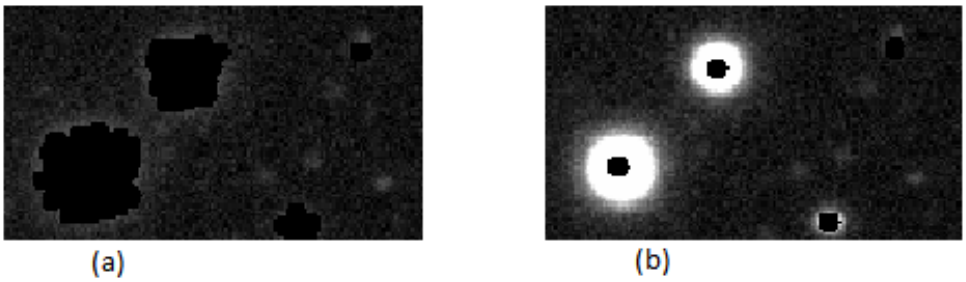

Figure 4: Black circles represent areas that have been treated as sources by the detection program. (a) shows those detected before code was added telling the program to ignore aperture areas which already contained a zero value. (b) shows sources detected after this section of code was added. As can be seen, there are some sources which aren't contained by the aperture.

As the aperture size is increased, more than one source is likely to be contained within a single aperture. Thus an appropriate size would be a compromise. The mean source area is 51 pixels, suggesting an aperture radius of 4 pixels ($\pi \times 4^2 \approx 51$)may be a reasonable compromise. However, as some of the sources are much larger than this, the number counts may be skewed - if lots of apertures fit inside one large source, this will give rise to a jump in the frequency distribution in the range of brightnesses contained in the source.

An aperture of recommended radius 6 pixels[1] was used as a starting point (corresponding to 3" diameter), centred on the maximum value. A larger-radius annular aperture was then placed around this to calculate the background level local to each source, which was then subtracted from the source aperture value. Different radii were breifly compared, including a radius of 4 pixels (2" diameter).

Due to the extensive limitations of the fixed aperture method, a variable aperture method was developed and the results looked at in more detail.

2.5 Variable Aperture Method

By making better use of inbuilt Matlab functions, the variable aperture is much more effective at quickly detecting and analysing sources (it runs in about 3 seconds).

'Thresholding' was used to segment the image based on pixel counts - the image was converted to a binary image, in which any pixels with a count higher than the source/background threshold (as determined above) become ones, the rest zeros. By assigning distinct labels to each separate region

of ones, Matlab was then able to run through them sequentially, analysing each corresponding source and local background as it went. An issue with this is that sometimes part of the source becomes 'disconnected' from the main section (as can be seen in the top left and bottom right sides of the binary image in figure 5).

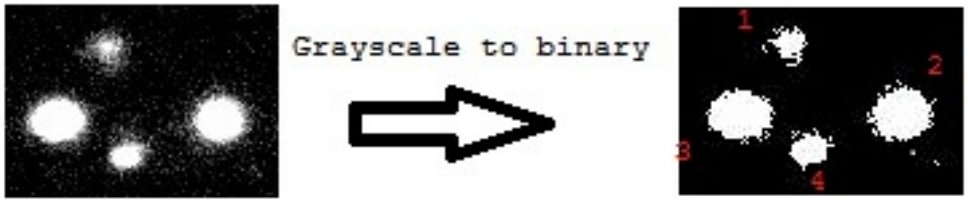

Figure 5: A section of the image in grayscale, and the same section in binary, showing that a good approximation of the source shape and area is obtained. However, notice the small white areas near sources 1 and 2. These are counted as separate sources, regardless of whether they are legitimate sources or disconnections from nearby sources.

These disconnections may lead to an excess of faint sources being detected.

Another issue arises with finding the local background for each source. To do so an area surrounding each source is looked at. If multiple sources are close together and their 'local background areas' overlap then the same local background, averaged over the regions local to each source, is used for all of these sources.

Despite these issues, the variable aperture method was the preferred method as it always analyses all of the sources in the image (so long as the threshold allows them all to be detected), and unlike the fixed aperture it analyses the actual shape and area of each source (again limited by the accuracy of the threshold used).

3 Results & Analysis

First the results of the fixed aperture method are briefly looked at, with different aperture sizes compared. Then the variable aperture method is looked at in more detail and finally the two sets of results are briefly compared. The raw photon counts are converted to magnitudes using the equation $m = ZP_{inst} - 2.5log_{10}(counts)$ where ZP_{inst} is the instrumental zero point, as determined in the AB magnitude system (in which 3631 Jy is defined to be zero magnitudes).

According to the fits header for the image the maximum reliable value for photon counts per CCD pixel is 36000 - for a one-pixel source this translates to magnitude 14. Although we have excluded single-pixel sources from our survey this suggests that for magnitude 14 and brighter more sources will have unreliable results, as determined by the limitations of the equipment used. This should be kept in mind when looking at the results.

3.1 Fixed Aperture

Number count against magnitude is plotted for various aperture radii. The 4-pixel radius appears to produce the straightest graph. This could imply that the 'wobbles' in the other graphs are due to the limits of a fixed aperture rather than physical phenomena.

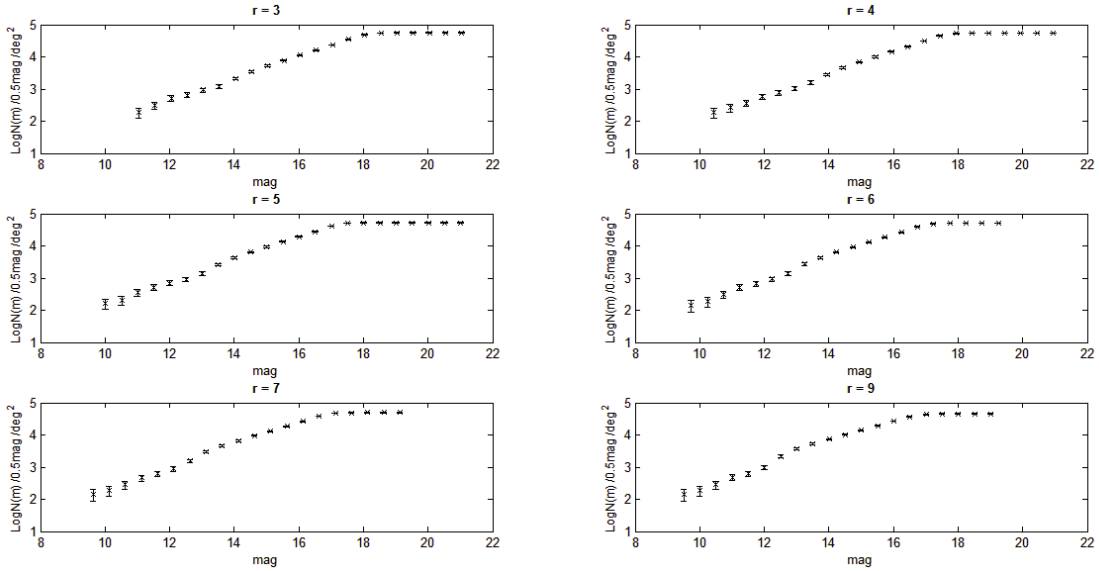

Figure 6: An aperture radius of 4 pixels has the 'straightest' graph. As the radius diverges from this the data points become more and more 'wobbly'. In all cases, just below magnitude 14 there was a dip in the graph.

3.2 Variable Aperture

Using a variable aperture 3404 sources are found in the magnitude range 9.3 to 23.6. The plot shows much more curvature than the fixed aperture graphs. This is expected as galaxies become gradually more difficult to detect at higher magnitudes, so the decreasing gradient represents the gradual increase of incompleteness in the survey. Excluding those sources which contain a pixel value of over 36000 (the maximum good data value as described by the fits header) has very little effect - only 14 sources are excluded and the resulting graph looks the same.

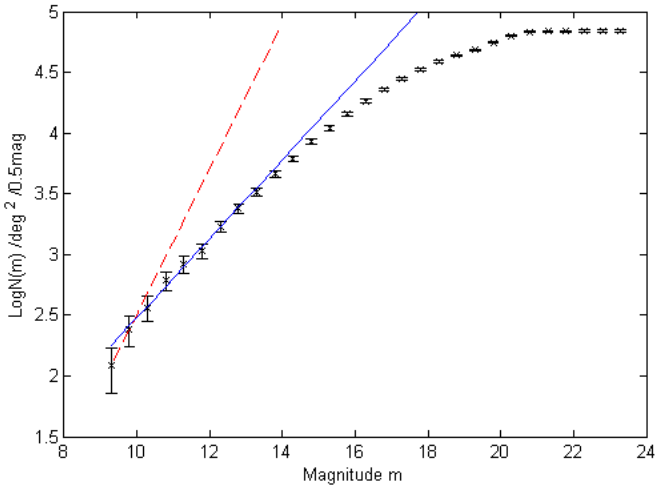

Figure 7: The errors shown are the errors in the number counts of galaxies following a poisson distribution. The solid line shows the gradient (0.34 ± 0.02) of the plot up to magnitude 13. The dashed line shows a gradient of 0.6, that predicted by equation 8. The errors in magnitude aren't included as they are too small to show up on the graph (see appendix for more details).

The gradient of the best fit line from the lowest detected magnitude up to 13 is 0.34 ± 0.02. As can be seen by the curvature of the graph this gradually decreases, reaching about 0.1 between 18 and 20, and it is finally zero (to one decimal place) between 21 and 23.

Even the maximum gradient of about 0.4 at the very start of the graph is much lower than the gradient of 0.6 predicted by equation 8. If the survey was complete, there would be an increase in the galaxy counts at higher magnitudes which would increase the gradient. Removing the brightest sources (which exhibited a blooming effect) also may have affected the gradient; low numbers of bright sources would increased the gradient.

Yasuda[5] et al (2001) present galaxy surveys with very high levels of completeness, in a variety of bands including r-band. At lower magnitudes, where effects of evolution and large-scale structure are less significant, their number counts fit equation 8 well. This supports the suggestion that our data may suffer from incompleteness - and that this effect worsens at increasing faintnesses.

4 Conclusion

As discussed the variable aperture is believed to be much more reliable in terms of detecting and collecting representative data on each source in the image. While the program using a fixed aperture gives results that are closer to those predicted by theory and found by other surveys, it is suspected that this is misleading - that perhaps the unquantified systematic errors in the fixed aperture actually caused the data to appear closer to the predictions than than it truely is. This fits the results found for the variable aperture, as it suggests high levels of incompleteness starting even at the brighter magnitudes.

Using a larger number of shorter exposures would improve the results for the brightest sources as fewer would need to be blacked out before analysis. However, this would reduce completeness at the fainter magnitudes. Alternatively using a better CCD (e.g. with a higher bit counter) would vastly improve the results - longer exposure times could be used allowing fainter sources to be detected more reliably, without causing as many pixels to saturate and bloom.

Another limitation is that the detecting programs can't distinguish between a) stars and galaxies, and b) two overlapping sources. Both issues may be addressable by looking at more detailed photometry for each source - for example, Yasuda et al (2001)[5] use a program called 'PHOTO' which looks for multiple peaks in each object and 'deblends' them into multiple 'child' objects. This program is also able to determine whether a source is likely to be a star or a galaxy based on its surface brightness profile (as described by Blanton et al, 2001[7]).

Overall, while there is room for improvement, the variable aperture program is deemed to be successful at identifying and analysing sources in the image. However, the incompleteness of the image has left us unable to make any reasonable physical conclusions regarding magnitude distribution among galaxies.

A Calculating Errors in Magnitude

The errors in magnitude are excluded from the graphs as they are very small - and in fact, none are large enough to affect the number of galaxies in each magnitude bin. They are approximated by treating the photon counts for each galaxy as a poisson distribution, with the error as the square root of the counts. These errors in counts are then converted into errors in magnitude, and finally added in quadrature with the zeropoint error included in the fits header file, to give the overall errors in magnitude for each galaxy. The largest error was 0.0227. As we are working with magnitude bins of 0.5, it's meaningless to talk about errors to 4 decimal places. To two decimal places, all of the errors are equal to 0.02, the value given for the zeropoint error.

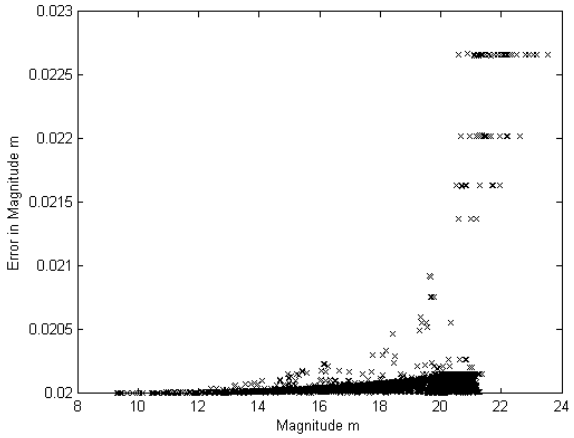

Figure 8: Distribution of errors with magnitude shows that although the errors are greatest for the faintest galaxies, all of the errors are very small.

References

[1] Clements, D. L., 2012, Computational Image Processing: A Deep Galaxy Survey [Lab script], 2012 ed., Imperial College London

[2] Raine, D. J., Thomas, E. G., 2002, An Introduction to The Science of Cosmology, 2nd ed., Bristol: Institute of Physics Publishing, p. 60

[3] Peacock, J. A., 1999, Cosmological Physics, Cambridge: Cambridge University Press, p. 73

[4] Maddox, S. J. et al, 1990, Galaxy Evolution at Low Redshift, Mon. Not. R. astr. Soc., 247, pp.1-5

[5] Yasuda, N., et al. 2001, Galaxy Number Counts From The Sloan Digital Sky Survey Commissioning Data, A.J., 122, pp. 1104-1124

[6] Eisenstein, D. J., et al. 2001, Spectroscopic Target Selection For The Sloan Digital Sky Survey: The Luminous Red Galaxy Sample, A.J., 122, pp. 2267-2280

[7] Blanton, M. R., et al. 2001, The Luminosity Function Of Galaxies In SDSS Commissioning Data, A.J., 121, pp. 2358-2380

[8] Sandage, A., 1961, The Ability of the 200-Inch Telescope to Discriminate Between World Models, Amer. Astr. Soc., 133, pp.335-392

[9] Caltech Astronomy, 2012. The 200 Inch Hale Telescope. [online] Available at `http://www.astro.caltech.edu/palomar/hale.html` [Accessed 4 November 2012].